

UCLA

UCLA Previously Published Works

Title

Amyloid β Protein: A β 40 Inhibits A β 42 Oligomerization

Permalink

<https://escholarship.org/uc/item/5wm847bj>

Journal

Journal of the American Chemical Society, 131(18)

ISSN

0002-7863

Authors

Murray, Megan M
Bernstein, Summer L
Nyugen, Vy
et al.

Publication Date

2009-05-13

DOI

10.1021/ja8092604

Peer reviewed

Amyloid β Protein: $A\beta_{40}$ Inhibits $A\beta_{42}$ Oligomerization

Megan M. Murray,[†] Summer L. Bernstein,[†] Vy Nyugen,[†] Margaret M. Condrón,[‡] David B. Teplow,[‡] and Michael T. Bowers^{*,†}

Department of Chemistry and Biochemistry, University of California, Santa Barbara, California 93106-950, and Department of Neurology, David Geffen School of Medicine, and Molecular Biology Institute and Brain Research Institute, University of California, Los Angeles, California 90095

Received December 5, 2008; E-mail: bowers@chem.ucsb.edu

The aggregation of the amyloid β protein ($A\beta$) is an important event in the development of Alzheimer's disease (AD).¹ Although $A\beta_{40}$ is ~ 10 times more abundant than $A\beta_{42}$ in vivo, $A\beta_{42}$ is the primary component of the amyloid deposits that are a hallmark of AD. Studies have also shown that $A\beta_{42}$ is significantly more neurotoxic than $A\beta_{40}$.² Chemical cross-linking studies have shown that while both $A\beta_{40}$ and $A\beta_{42}$ are capable of forming fibrils, they maintain distinct oligomer distributions.³ For example, $A\beta_{40}$ and $A\beta_{42}$ monomers form dimers, trimers, and tetramers in solution. $A\beta_{42}$, however, may also form pentamers and hexamers, called paranuclei, that self-associate to form dodecamers, protofibrils, and fibrils.³ In vivo studies in mice and humans suggest that dodecamers of $A\beta_{42}$ may be the proximate neurotoxins in AD.^{4,5}

Recently, new evidence has emerged from in vitro^{6,7} and in vivo⁸ studies showing that $A\beta_{40}$, in addition to its unique assembly characteristics relative to $A\beta_{42}$, may inhibit protofibril and fibril formation by the latter peptide. In this work, we used mass spectrometry coupled with ion mobility spectrometry (IMS)^{9–12} to elucidate potential mechanisms for the $A\beta_{40}$ effect. IMS has successfully been employed in the past to study the structure of $A\beta^{13,14}$ and fragments of $A\beta$.^{15,16} For this study, $A\beta_{40}$ and $A\beta_{42}$ were synthesized using Fmoc chemistry¹⁷ and dissolved separately in a 20 mM ammonium acetate buffer (pH 7.4) at a final concentration of 2 mg/mL. The solutions were combined in a 1:1 $A\beta_{40}/A\beta_{42}$ ratio and filtered using Macro Spin Column gel filters (The Nest Group, Inc.). The samples were analyzed on a home-built nano-ESI ion mobility mass spectrometer.¹⁸

The mass spectrum of a 1:1 mixture is given in Figure 1 [spectra and arrival time distributions (ATDs) for other mixtures are given in the Supporting Information (SI)]. Peaks corresponding to the $z/n = -4, -3, -5/2,$ and -2 charge states ($z = \text{charge}, n = \text{oligomer size}$) are present for both $A\beta_{40}$ and $A\beta_{42}$. A third peak is present between the $z/n = -5/2$ peaks for $A\beta_{40}$ and $A\beta_{42}$. This peak (m/z 1770) represents the $-5/2$ peak for a mixed oligomer containing equal parts $A\beta_{40}$ and $A\beta_{42}$. For a 1:1 mixture, nearly equal intensities are expected for the $A\beta_{40}$ and $A\beta_{42}$ monomer peaks ($z/n = -4$ and -3), but clearly the $A\beta_{40}$ peaks are much larger than the $A\beta_{42}$ peaks. This result is consistent with the fact that pure $A\beta_{42}$ oligomerizes much more rapidly than $A\beta_{40}$, leading to depletion of $A\beta_{42}$ monomer, and that large aggregates of $A\beta_{42}$ often clog the nano-ESI spray tip in our experiments. In addition, a 1:2:1 distribution is expected for the $z/n = -5/2$ dimer peaks, but again, the $A\beta_{42}$ -dependent peaks are depleted, supporting the conclusion that rapid $A\beta_{42}$ aggregation has occurred (see the SI).

IMS makes possible the separation of species that have the same mass-to-charge ratio but differ in shape or size. For IMS separation, the ions pass through a drift cell filled with helium gas (~ 5 Torr)

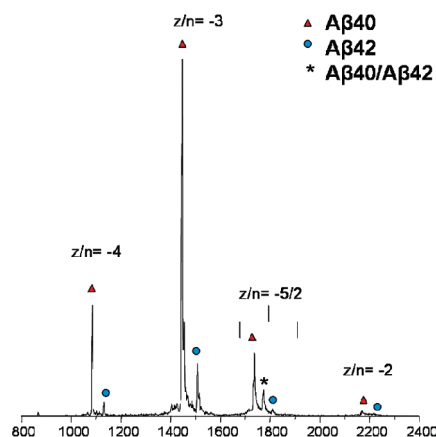


Figure 1. Negative-ion mass spectrum of the 1:1 mixture of $A\beta_{40}$ and $A\beta_{42}$.

under the influence of a weak electric field, E . This allows species to be separated in time according to their cross sections. If the ions are pulsed into the drift cell, their arrival times at the detector can be measured. Measurements of the ATDs are given in Figure 2 for the three $z/n = -5/2$ peaks in the mass spectrum.

The $A\beta_{40}$ peak is shown in Figure 2a and is composed of two partially resolved features. The smallest possible oligomer at $z/n = -5/2$ is the $z = -5$ dimer. Injection energy studies (data not shown; see ref 13 for a detailed discussion of injection energy methods) indicate that the feature at longer times (500–525 μs) is strongly favored at high injection energies. Since no new features appear at longer times at the highest injection energies, this peak can be assigned as the $z = -5$ dimer. At the lowest possible injection energies, the shorter time feature (near 430 μs) is favored. Higher-order oligomers with the same value of z/n as lower-order oligomers always appear at shorter arrival times,¹³ allowing the 430 μs feature to be assigned as the $z = -10$ tetramer. No other peaks appear in the $A\beta_{40}$ $z/n = -5/2$ ATD, so under the conditions of our experiment, oligomerization stops at the tetramer.

The ATD for the $z/n = -5/2$ peak of pure $A\beta_{42}$ is given in Figure 2b. Clearly, this ATD is more complex than that of $A\beta_{40}$. Again, the various features were assigned previously using injection energy studies.¹³ In addition, molecular modeling was performed to assign the qualitative structure of each of the peaks,¹⁹ as noted in the figure. Of interest is the fact that $A\beta_{42}$ forms a planar cyclic hexamer (a paranucleus), which was previously shown to exist in the $A\beta_{42}$ oligomer distribution but not in the $A\beta_{40}$ distribution. This structure is crucial for subsequent oligomerization of $A\beta_{42}$.³ Also of interest is the terminal $(A\beta_{42})_{12}$ species at ~ 350 μs , a dodecamer formed by stacking of two planar hexamer rings.¹⁹ The dodecamer has been implicated in memory impairment in transgenic mice^{4,20} and in human AD.⁵

[†] University of California, Santa Barbara.

[‡] University of California, Los Angeles.

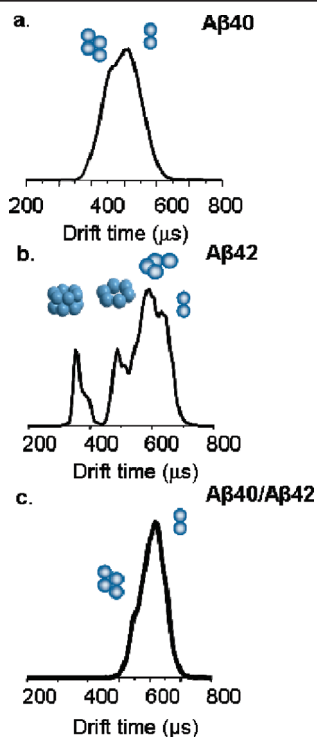
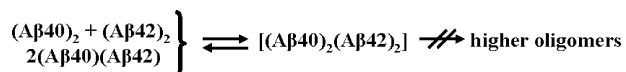


Figure 2. ATDs for the $z/n = -5/2$ charge states of (a) $A\beta_{40}$, (b) $A\beta_{42}$, and (c) $A\beta_{40}/A\beta_{42}$.

The ATD for the mixed oligomer (1:1 $A\beta_{40}/A\beta_{42}$) is given in Figure 2c and shows two incompletely resolved features. Injection energy studies (not shown) indicate that the longer time peak ($\sim 600 \mu\text{s}$) is strongly favored at the highest injection energies while the shorter time peak ($\sim 490 \mu\text{s}$) becomes more prominent at lower injection energies. These two features are the only ones observed. We assign the $\sim 600 \mu\text{s}$ peak as the $z = -5$ mixed dimer [$(A\beta_{40})(A\beta_{42})$] and the $\sim 490 \mu\text{s}$ peak as the $z = -10$ mixed tetramer [$(A\beta_{40})_2(A\beta_{42})_2$].

Formation of mixed tetramers with 3:1 or 1:3 $A\beta_{40}/A\beta_{42}$ ratios may be possible, but they are not observed in the mass spectrum (Figure 1). This result supports the formation of the mixed tetramer via dimer condensation rather than sequential monomer addition:



The second and most important aspect of the mixed oligomer ATD in Figure 2c is that no species larger than tetramers are

observed. What this suggests is that $A\beta_{40}$, which is present at ~ 10 times the concentration of $A\beta_{42}$ in a healthy human brain, actually sequesters $A\beta_{42}$ in stable mixed tetramers, thereby preventing further oligomerization of $A\beta_{42}$ to form the putative dodecamer toxic agent and consequently potentially deterring the development of AD.

Acknowledgment. The support of the National Institutes of Health under Grant IPOIAG027818 is gratefully acknowledged.

Supporting Information Available: Additional mass spectra of mixtures of different ratios as well as ATDs from the injection energy study of the $z/n = -5/2$ peak. This material is available free of charge via the Internet at <http://pubs.acs.org>.

References

- (1) Roychoudhuri, R.; Yang, M.; Hoshi, M. M.; Teplow, D. B. *J. Biol. Chem.* **2009**, *284*, 4749–4753.
- (2) Dahlgren, K. N.; Manelli, A. M.; Stine, W. B.; Baker, L. K.; Krafft, G. A.; LaDu, M. J. *J. Biol. Chem.* **2002**, *277*, 32046–32053.
- (3) Bitan, G.; Kirkitadze, M. D.; Lomakin, A.; Vollers, S. S.; Benedek, G. B.; Teplow, D. B. *Proc. Natl. Acad. Sci. U.S.A.* **2003**, *100*, 330–335.
- (4) Lesne, S.; Koh, M. T.; Kotilinek, L.; Kaye, R.; Glabe, C. G.; Yang, A.; Gallagher, M.; Ashe, K. H. *Nature* **2006**, *440*, 352–357.
- (5) Klein, W. L.; Stine, W. B.; Teplow, D. B. *Neurobiol. Aging* **2004**, *25*, 569–580.
- (6) Jan, A.; Gokce, O.; Luthi-Carter, R.; Lashuel, H. A. *J. Biol. Chem.* **2008**, *283*, 28176–28180.
- (7) Yan, Y. L.; Wang, C. Y. *J. Mol. Biol.* **2007**, *369*, 909–916.
- (8) Kim, J.; Onstead, L.; Randle, S.; Price, R.; Smithson, L.; Zwizinski, C.; Dickson, D.; Golde, T.; McGowan, E. *J. Neurosci.* **2007**, *27*, 627–633.
- (9) Bowers, M. T.; Kemper, P. R.; Vonhelden, G.; Vankoppen, P. A. M. *Science* **1993**, *260*, 1446–1451.
- (10) Clemmer, D. E.; Jarrold, M. F. *J. Mass Spectrom.* **1997**, *32*, 577–592.
- (11) Wyttenbach, T.; Bowers, M. T. *Mod. Mass Spectrom.* **2003**, *225*, 207–232.
- (12) Vonhelden, G.; Hsu, M. T.; Kemper, P. R.; Bowers, M. T. *J. Chem. Phys.* **1991**, *95*, 3835–3837.
- (13) Bernstein, S. L.; Wyttenbach, T.; Baumketner, A.; Shea, J. E.; Bitan, G.; Teplow, D. B.; Bowers, M. T. *J. Am. Chem. Soc.* **2005**, *127*, 2075–2084.
- (14) Baumketner, A.; Bernstein, S. L.; Wyttenbach, T.; Bitan, G.; Teplow, D. B.; Bowers, M. T.; Shea, J. E. *Protein Sci.* **2006**, *15*, 420–428.
- (15) Murray, M.; Krone, M.; Bernstein, S.; Wyttenbach, T.; Condrion, M.; Teplow, D. B.; Shea, J.; Bowers, M. T. Submitted for publication.
- (16) Wu, C.; Murray, M.; Bernstein, S.; Condrion, M.; Bitan, G.; Shea, J.-E.; Bowers, M. T. *J. Mol. Biol.* **2009**, *387*, 492–501.
- (17) Lomakin, A.; Chung, D. S.; Benedek, G. B.; Kirschner, D. A.; Teplow, D. B. *Proc. Natl. Acad. Sci. U.S.A.* **1996**, *93*, 1125–1129.
- (18) Wyttenbach, T.; Kemper, P. R.; Bowers, M. T. *Int. J. Mass Spectrom.* **2001**, *212*, 13–23.
- (19) Bernstein, S. L.; Dupius, N. F.; Lazo, N. D.; Wyttenbach, T.; Condrion, M.; Bitan, G.; Teplow, D. B.; Shea, J.-E.; Ruotolo, B. T.; Robinson, C. V.; Bowers, M. T. Submitted for publication.
- (20) Cheng, I. H.; Searce-Levie, K.; Legleiter, J.; Palop, J. J.; Gerstein, H.; Bien-Ly, N.; Puolivali, J.; Lesne, S.; Ashe, K. H.; Muchowski, P. J.; Mucke, L. *J. Biol. Chem.* **2007**, *282*, 23818–23828.

JA8092604